RESIDUAL STRESS MEASUREMENT USING INDENTATION AND A RADIAL IN-PLANE ESPI INTERFEROMETER

Ricardo Sutério, Armando Albertazzi G. Jr, Felipe K. Amaral, Anderson Pacheco.

Universidade Federal de Santa Catarina, Cx. Postal 5053, CEP 88040-970, Florianópolis, SC, Brazil, albertazzi@labmetro.ufsc.br

ABSTRACT

A radial in-plane electronic speckle pattern interferometer (ESPI) has been developed by the authors' group. This interferometer is used in this paper to measure residual stresses in combination with the indentation method. A semi-empirical mathematical model is developed to quantify the residual stresses. Several tests were made in a specimen with different levels of residual stresses imposed by a mechanical loading. Empirical constants were computed from those tests and are used in combination with the developed model to predict the residual stresses levels. The radial displacement field around a controlled indentation print is measured, processed and fitted to a mathematical model to predict residual stresses. Series of tests were designed and executed. Different indentation tip geometry and different loading conditions were involved. This paper presents the measurement principle, implementation details and results of the performance evaluation. The tests presented here are not complete since they are restricted to only one material, one-axis stress state, two indentation tip geometry and only one indentation force, but they are sufficient to encourage further development.

Keywords: residual stress, indentation, ESPI; radial interferometer.

INTRODUCTION

A new kind of electronic speckle pattern interferometer (ESPI) has been developed by the authors' group using conical mirrors to achieve radial in-plane sensitivity[1]. This device has been used for several applications on the field of experimental mechanics[6],[7],[8]. In this paper this radial in-plane (RIP) is used in combination with the indentation method to measure residual stresses.

To measure residual stresses a controlled indentation print is applied to the surface of the specimen by a conical diamond and spherical tip. As a consequence, a local yielding is developed and the material on the specimen surface moves away from the indentation print. The amount of the radial displacement component around the indentation print is influenced by the level and direction of residual stresses state acting in the specimen.

In many applications, it is very important to know the magnitude and direction of residual stresses. Since residual stresses are very difficult to be predicted using analytical or numerical models, their values are very often determined by direct measurement by experimental methods. One of the most widely used experimental methods is the hole-drilling technique. This technique involves monitoring the strains produced when a small hole is drilled into a stressed material. The drilled hole produces a local release of residual stresses that are measured by a special type of strain gauges. Those values are used into an appropriate mathematical method to quantify the residual stresses level[4].

Alternatively, it is possible to obtain qualitative information about the residual stresses acting in a material by the indentation method[8],[9]. The main idea is to produce a local indentation print using a tool with a conical or spherical tip and a controlled level of loading or total energy. In opposition to the hole drilling method, the indentation does not release stresses but add more stresses creating a local plastic zone. The local plastic deformation is a function of the geometry of the indentation tip, material properties, and is also strongly dependent of the magnitude and direction of the

Eighth International Symposium on Laser Metrology, edited by R. Rodriguez-Vera, F. Mendoza-Santoyo, Proc. of SPIE Vol. 5776 (SPIE, Bellingham, WA, 2005)
0277-786X/05/$15 · doi: 10.1117/12.611629

residual stresses initially present in the material. Previous works had reported different attempts to quantify residual stresses using the indentation method from: (a) hardness variation measurement; (b) relation between force and indentation depth; (c) the final geometric shape of the indentation print and (d) deformation or displacement measured around the indentation print[2],[3],[8] [9] . This behavior is very difficult to be analytically and numerically modeled and it is not usually used for quantitative measurement in a very accurate way.

Results of a quantitative evaluation of residual stresses measurement using indentation is reported in this paper. An indentation print is produced in the region where residual stresses have to be measured. The in-plane radial displacement is measured around it. There is a clear correlation between the residual stresses level and the fringe pattern developed around the indentation print. A semi-empirical mathematical model was developed using the hole drilling model as a starting point. Additional parameters where added to this model to best represent the actual measured data. The possibilities to use those additional parameters to quantify the residual stresses are here investigated.

THE RADIAL INTERFEROMETER

A double illumination radial in-plane interferometer (RIP) using ESPI is used in this paper[1]. The basic principle is shown in Figure 1. This interferometer was recently incorporated in a portable and modular device for residual stresses measurement.

The main optical element of the interferometer is a conical mirror, which is placed near the specimen surface. Figure 1(a) shows a cross-section of the conical mirror containing the mirror axis, which displays two particularly chosen light rays from a collimated illumination source. Each light ray is reflected by the conical mirror surface towards a point P over the specimen surface, reaching this point symmetrically. The illumination directions are indicated by the unitary vectors nA and nB and they have the same angle with respect to the surface normal. The sensitivity direction is given by the vector k obtained from the subtraction of the two unitary vectors. Therefore, in-plane sensitivity is reached in point P as well as in any other point on the circular double illuminated area. The only exception is the central point, there is a singular point.

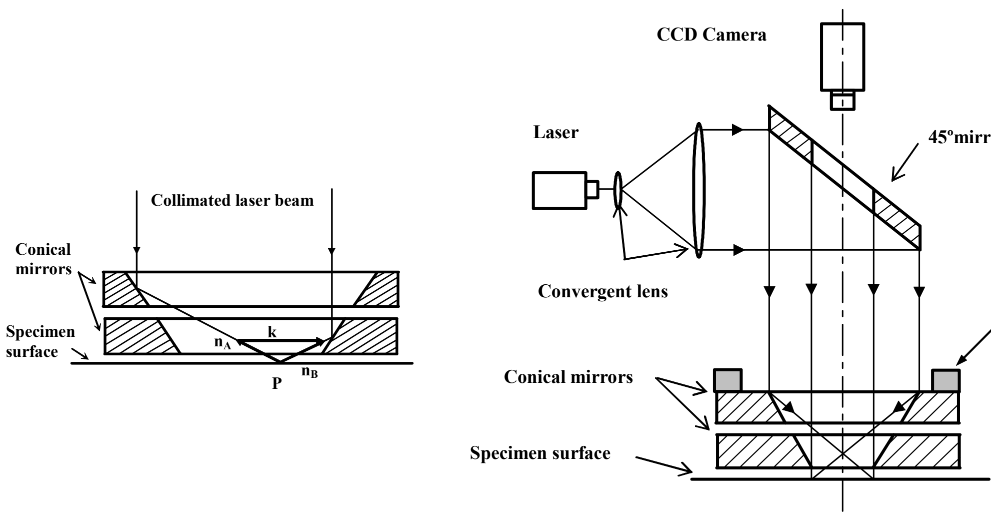

(a) (b)

Figure 1: Double illumination through the radial interferometer.

A practical configuration of the radial in-plane interferometer is shown in Figure 1(b). The laser light is expanded and collimated. The collimated beam is reflected towards the conical mirror using a 45º tilted mirror. The central circular window located at this mirror has two main functions: (a) to avoid that the laser light to reach directly the measured surface to prevent triple illumination, and (b) to provide a viewing window for the camera. The conical mirror is formed by two parts with a small gap between them that is controlled by a PZT actuator do produce phase shifting.

Figure 2 shows two examples of phase differences patterns.

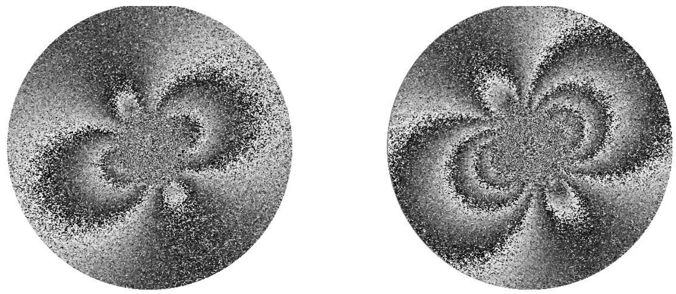

Figure 2: Typical phase diference patterns for two different residual stresses levels.

This radial displacement field is accurately measured by the RIP interferometer. The phase pattern is processed and few parameters are extracted. An appropriate mathematical model was developed and is used to quantify the residual stresses levels.

RESIDUAL STRESS MEASUREMENT

In order to measure residual stresses usually a small hole is drilled in the center of the measured area. A mathematical model developed by Kirsch[4] based on the elastic solution for an infinite plate, subjected to a uniform state of stresses, with a cylindrical hole drilled all way through the plate thickness, is used. According to that, the radial component of the displacement field (u_r), developed by the hole drilling in polar coordinates is[1],[5]:

$$u_r(\rho,\theta) = A(\rho)(\sigma_1+\sigma_2) + B(\rho)(\sigma_1-\sigma_2)\cos(2\theta-2\beta) \tag{1}$$

where the functions A(ρ) and B(ρ) are given by:

$$A(\rho) = \frac{(1+\upsilon)}{2E} r_0\,\rho \qquad B(\rho) = \frac{1}{2E} r_0 \left[4\rho - (1+\upsilon)\rho^3\right] \tag{2}$$

and,
- r, θ — *are polar coordinates;*
- r_o — *is the drilled hole radius;*
- ρ — *is the normalized radius ($\rho = r_0 / r$);*
- σ_1, σ_2 — *are the principal residual stresses (maximum and minimum respectively);*
- E — *is the material's Young modulus;*
- υ — *is the material's Poisson ratio;*
- β — *is the principal direction angle.*

Figure 3(a) shows a typical radial phase difference pattern for a one-axis residual stress state due to hole drilling method combined with ESPI. The hole diameter is 0.8 mm and the residual stress is about 200 MPa.

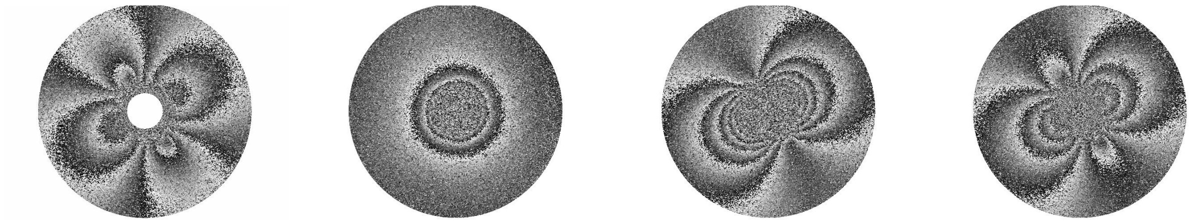

(a) (b) (c) (d)

Figure 3: Typical phase patterns of the radial displacement fields component:
(a) for Holing Drilling Method (computer simulated), (b) in a stress-free material after indentation,
(c) with 200 MPa stress after indentation, and (d) phase difference: (c - b)

In opposition to the hole drilling method, the indentation print does not release the stresses, but add more stresses, producing a local yielding. As a consequence, a permanent displacement field is produced around it. In a stress-free material, this permanent displacement field is axi-symmetrical and repeatable if the indentation tip geometry, indentation loading and material properties are constant. If mechanical or residual stresses are present in the material prior the indentation, the permanent displacement field is affected in a way that depends on the residual stresses levels.

Figure 3(b) to (d) show some experimental results. Those phase difference patterns are related to the radial displacement component, measured by the radial in-plane ESPI interferometer. The indentation was made using a 120^o conic tip. Figure **3**(b) shows the radial displacement in a stress-free material. Figure 3(c) shows the radial displacement in a material with a one-axis 200 MPa stresses field aligned about 30° with the horizontal axis, and Figure 3(d) shows the resulting phase difference between the two previous phase patterns.

Comparing Figure 3(a) and Figure 3(d) it is possible to see that, after removing the permanent displacement field related to an indented stress-free material, there is a strong similarity between them.

MATHEMATICAL MODEL

In order to find a model to measure residual stresses the authors' approach uses this similarity. A mathematical model was derived starting from equation (1). It is noted that the term that depend on *cos(2θ)* is related to the principal stresses difference $(\sigma_1 - \sigma_2)$ and the term independent of θ is related to the principal stresses sum $(\sigma_1 + \sigma_2)$. The radial component of the displacement field (u_r), is here modeled in polar coordinates by the following equation:

$$u_r(r,\theta) = \frac{K_1}{r} + \left(\frac{K_2}{r} + \frac{K_3}{r^3}\right)\cos(2\theta - 2\beta) \qquad (3)$$

where K1, K2 and K3 are unknown functions given by:

$$K_1 = f[(\sigma_1 + \sigma_2), E, \upsilon] \qquad K_2 = g[(\sigma_1 - \sigma_2), E, \upsilon] \qquad K_3 = h[(\sigma_1 - \sigma_2), E, \upsilon] \qquad (4)$$

It was experimentally verified that the radial displacement on a stress-free material can be reasonably described using the equation proposed by Giannakopoulos & Suresh - 1997[2]:

$$u_r(r) = C\frac{\upsilon}{E(\upsilon - 1)}\frac{1}{r^{\frac{1}{\upsilon}-1}} \qquad (5)$$

Where, C is a constant that depends upon the indentation force, tip geometry and materials properties.

This constant can be determined by fitting this model to experimental data from the radial displacement field measured after indenting a stress-free specimen of the same material in identical indentation conditions. So, our model to relate residual stress with the radial displacement field is given by:

$$u_r(r,\theta)=\frac{K_1}{r}+\left(\frac{K_2}{r}+\frac{K_3}{r^3}\right)\cos(2\theta-2\beta)+K_4\,\frac{1}{r^{\frac{1}{\upsilon}-1}} \tag{6}$$

Where K_4 depends of C, E and υ, as it is clear in equation (5), and can be determined a priori in a stress-free specimen.

In a recent investigation[6] the authors verfied that the term K_3 / r^3 in equations (3) and (6) is negligible if compared with K_2 / r. So, equations (3) and (6) can be simplified and rewritten as:

$$u_r(r,\theta)=\frac{K_1}{r}+\frac{K_2}{r}\cos(2\theta-2\beta) \tag{7}$$

$$u_r(r,\theta)=\frac{K_1}{r}+\frac{K_2}{r}\cos(2\theta-2\beta)+\frac{K_4}{r^{\frac{1}{\upsilon}-1}} \tag{8}$$

Equation (7) is applied when the radial displacement field from a stress-free specimen is subtracted from the radial displacement field measured for a specimen with residual stresses. By the other hand, the authors wish to investigate if equation (8) can be successfully used to quantify residual stresses without removing the radial displacement field from a stress-free specimen. So, the constant K_4 must be fitted using the actual total radial displacement field.

In order to try to keep those equations material independent, they were again rewritten as equations below. This independence must be experimentally verified in a future work.

$$u_r(r,\theta)=\frac{(1+\upsilon)}{2E}\,\frac{1}{r}\,\psi_1\;+\;\frac{2}{E}\,\frac{1}{r}\;\psi_2\;\cos(2\theta-2\beta) \tag{9}$$

$$u_r(r,\theta)=\frac{(1+\upsilon)}{2E}\,\frac{1}{r}\,\psi_1\;+\;\frac{2}{E}\,\frac{1}{r}\;\psi_2\;\cos(2\theta-2\beta)\;+\;\frac{\upsilon}{E(\upsilon-1)}\,\frac{1}{r^{\frac{1}{\upsilon}-1}}\,\psi_3 \tag{10}$$

Where ψ_1, ψ_2 and ψ_3 are constants that depend upon the indentation force and tip geometry. Additionally, ψ_1 is also a function of $\sigma_1 + \sigma_2$ and ψ_2 is a function of $\sigma_1 - \sigma_2$.

EXPERIMENTAL SETUP

Figure 4(a) shows the portable ESPI radial in-plane interferometer used in this work. The system is composed by a diode laser source with 658 nm wavelength, a 30° conical mirror and a CCD camera. The illuminated region is about 10 mm in diameter (Figure 4b).

The indentation module always applied the same level of constant impact energy. Two different tip geometries were used: a 120^{o} conical diamond tip and a 2.5 mm diameter spherical tungsten carbide tip (see Figure 5).

It is very difficult to evaluate the measurement performance of a residual stresses measurement device. Since there is no available reference standard, or even a reference measurement system, the authors applied a known mechanical stresses level in a previously annealed specimen. That approach mechanically simulates a known residual stresses state and it was sufficiently good for a first measurement performance evaluation. In order to overcome this difficulty, known residual stresses fields were mechanically simulated by the device shown in Figure 4(a). Basically, a long residual-stresses free specimen is loaded by traction through 6 bolts connected to a "U" shaped structure.

The specimen is a rectangular AISI 1020 steel bar with approximate dimensions of 3 x 50 x 3000 mm (Figure 6b). The long specimen was instrumented with ten strain gages to monitoring the actual tension level applied to the specimen in order to guarantee uniform loading and to provide a reference value for it. The specimen size is long enough to accommodate over 300 measurement points. The portable radial in-plane interferometer was clamped to the loading device in such a way that its measurement axis was aligned in about 30° with the loading direction.

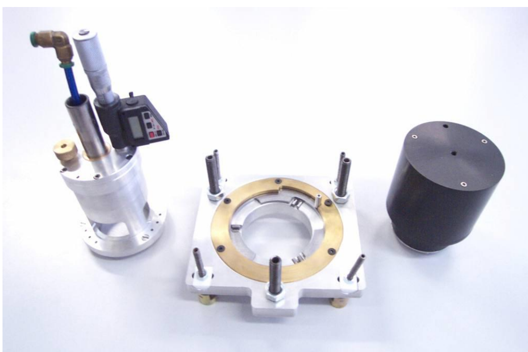

(a) Hole drilling module, universal base, and radial in-plane interferometer.

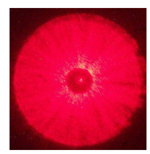

(b) Measurement area with 10 mm in diameter

Figure 4: Portable ESPI radial in-plane interferometer used in this work.

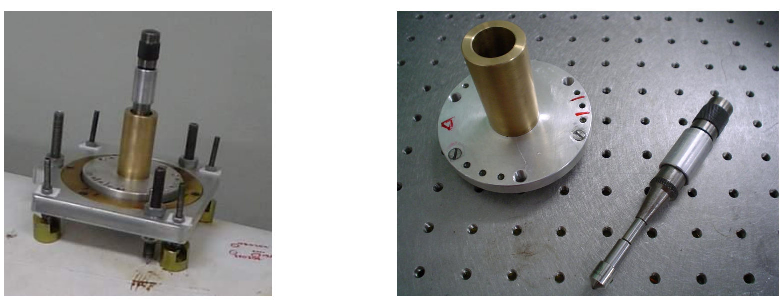

Figure 5: Indentation module with a 120° conical diamond or a 2.5 mm diameter spherical tungsten carbide tips.

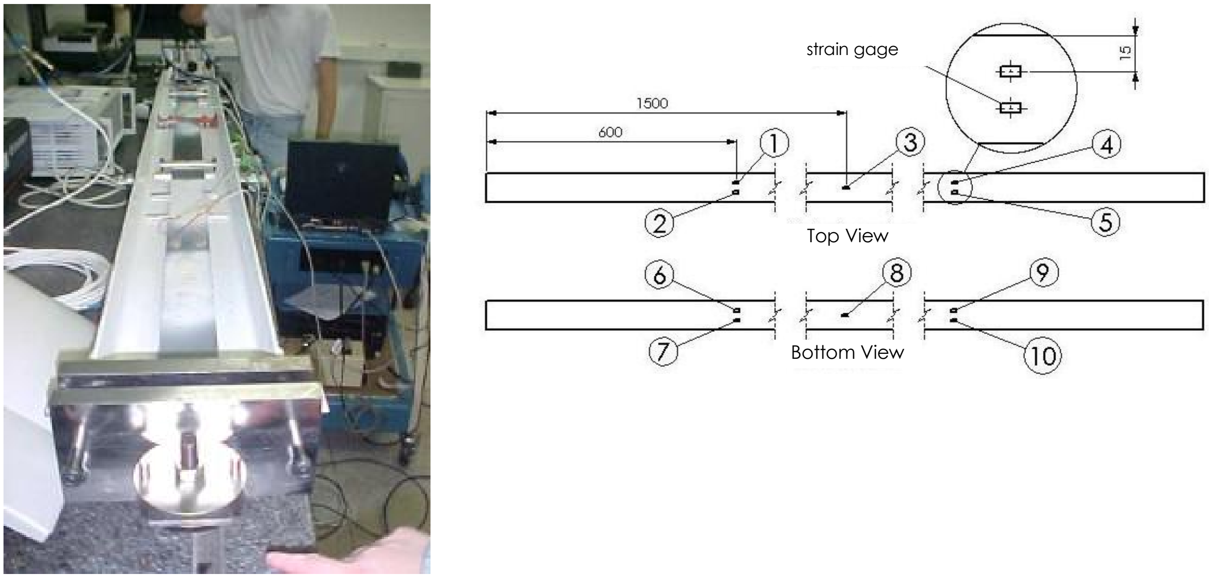

Figure 6: Loading system, specimen, and strain gages configuration.

EXPERIMENTAL RESULTS

A set of measurement tests was designed and executed with nine different stresses levels. For each stress level the same long specimen was indented three times. Both 120° conic tip and 2.5 mm spherical indentation tips were used applying about the same amount of energy given by a mechanical impact of a sphere driven by a spring at constant compression rate. So, a total of six images were acquired for each loading level.

Figure 7(a) to Figure 7(d) show different experimentally obtained images. A 229 MPa one-axis stresses filed was applied in the long specimen. The two kinds of indentation tips were used.

Test at 229 MPa, 120° conical tip		Test at 229 MPa, 2.5 mm spherical tip	
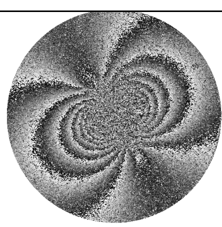	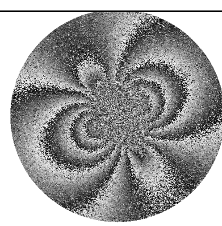	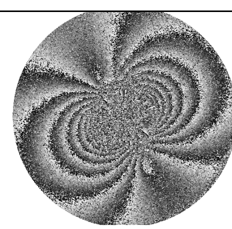	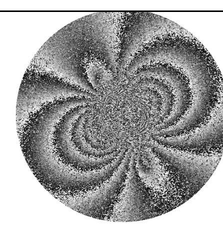
(a) total phase difference after indentation in a loaded material.	(b) phase difference: loaded material minus a stress-free material.	(c) total phase difference after indentation in a loaded material.	(d) phase difference: loaded material minus a stress-free material.

Figure 7: Typical test results for two indentation tips.

The measurement sampling region was delimited by two concentric circles with radius 1.5 and 4.5 mm. A polar mesh of 12 x 360 = 4320 sampling points was used in all calculations. In each case the reference values were given by the strain gauges with an uncertainty ranging from 5 to 9% with 95% confidence level[7].

In this paper the emphasis was given to investigate if is it possible to successfully quantify the residual stresses level without removing the radial displacement field of stress-free indentation. This goal is motivated by practical aspects.

Table 1 and Table 3 present measurement results. The first column is the reference stress level. Coolum two shows the relative stress related to material's yield point. The remaining columns present the parameters ψ_1, ψ_2 and ψ_3, fitted by least squares from the radial displacement data for each image.

Figure 8 and Figure 9 plot the dependence between ψ_1, ψ_2 and the reference stress level. Two quadratic polynomials, named $H(\sigma_1+\sigma_2) = \psi_1$ x $(\sigma_1+\sigma_2)$ and $\Gamma(\sigma_1-\sigma_2) = \psi_2$ x $(\sigma_1-\sigma_2)$, were fitted to the experimentally computed values, as show equations (11) to (14). In this particular case both sum and difference of principal stresses are equal since $\sigma_2 = 0$. ψ_3 did not show a correlation with the applied stresses. Its value is more correlated to the indentation energy that, ideally, should be kept constant.

Table 1: Parameters ψ_1 trough ψ_3 determined using least square fitting for 120° diamond cone tip.

σ_{ref} [MPa]	σ_{ref} / σ_y [%]	ψ_1	ψ_2	ψ_3
0.0	0.0%	97.30	7.32	-632
29.8	10.1%	99.35	9.83	-652
58.1	19.7%	134.56	18.49	-574
89.2	30.2%	162.46	34.61	-610
116.9	39.6%	230.35	51.99	-625
145.7	49.4%	200.60	68.33	-656
177.3	60.1%	232.48	83.87	-660
205.0	69.5%	319.38	111.58	-673
229.3	77.7%	434.14	143.37	-763

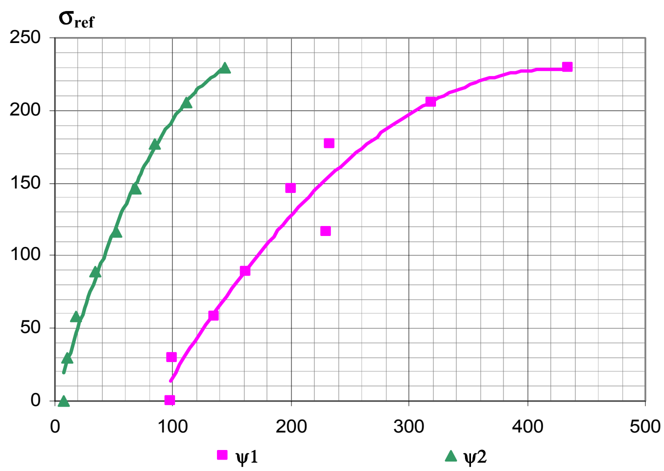

Figure 8: Indentation parameter versus reference residual stress for 120° diamond cone tip.

Quadratic regression shows a quite good agreement with experimental data. The correlations of *H* and *Γ* functions are better than 0.95 (R^2). From those predicted values, σ_1 and σ_2 can be computed by: $\sigma_1 = (H + \Gamma) / 2$ and $\sigma_2 = (H - \Gamma) / 2$. The resulting computed values for σ_1 and σ_2 are presented in Table 2 and Table 4 respectively.

$$H(\sigma 1+\sigma 2) = -0.0020008\ \psi_1^2 + 1.6999654\ \psi_1 - 132.5462366 \quad (R^2 = 0.9501378) \tag{11}$$

$$\Gamma(\sigma 1-\sigma 2) = -0.0079437\ \psi_2^2 + 2.7347403\ \psi_2 \quad (R^2 = 0.9887385) \tag{12}$$

Table 2: Predict stresses values for a 120° diamond cone tip.

Ref. Value [MPa]	Relative to Yield Point	Predict Values		Difference Error	
σ_{ref} [MPa]	σ_{ref} / σ_y	σ_1 [MPa]	σ_2 [MPa]	$\sigma_{ref} - \sigma_1$ [MPa]	$(\sigma_{ref} - \sigma_1) / \sigma_{ref}$
0.0	0.0%	16.8	-2.8	-16.8	--
29.8	10.1%	21.4	-4.8	8.5	28.4%
58.1	19.7%	53.9	6.1	4.2	7.2%
89.2	30.2%	88.0	2.8	1.3	1.4%
116.9	39.6%	136.8	16.1	-19.9	-17.1%
145.7	49.4%	138.9	-10.9	6.9	4.7%
177.3	60.1%	164.0	-9.5	13.3	7.5%
205.0	69.5%	206.3	0.0	-1.3	-0.6%
229.3	77.7%	228.6	-0.2	0.7	0.3%

Table 3: Parameters ψ_1 trough ψ_3 determined using least square fitting for 2.5 mm diameter tungsten carbide spherical tip.

σ_{ref} [MPa]	σ_{ref} / σ_y [%]	ψ_1	ψ_2	ψ_3
0.0	0.0%	177.87	5.15	-1045
29.8	10.1%	204.51	13.25	-956
58.1	19.7%	259.65	26.44	-884
88.7	30.1%	281.36	56.71	-920
116.9	39.6%	344.64	80.03	-1032
145.8	49.4%	373.43	101.91	-863
177.1	60.0%	419.67	122.39	-777
204.8	69.4%	497.05	154.62	-731
228.7	77.5%	666.32	201.99	-769

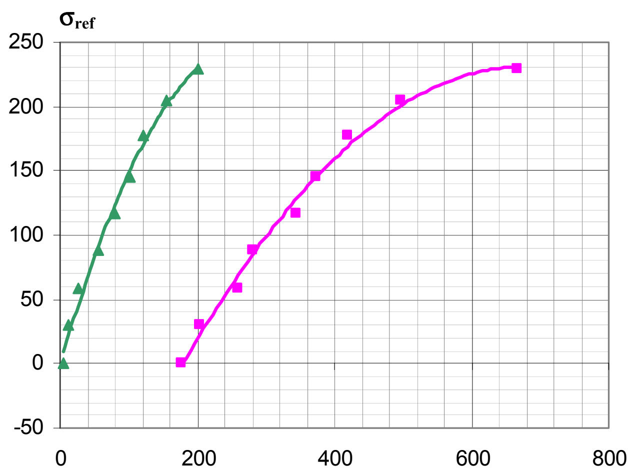

Figure 9: Indentation parameter versus reference residual stress for 2.5 mm diameter tungsten carbide spherical tip.

$$H1(\sigma 1+\sigma 2) = -0.0009301\ \psi_1^2 + 1.2604847\ \psi_1 - 195.8968010 \quad (R2 = 0.9924187) \tag{13}$$

$$\Gamma 2(\sigma 1-\sigma 2) = -0.0033273\ \psi_2^2 + 1.8136312\ \psi_2 \quad (R2 = 0.9919385) \tag{14}$$

Table 4: Predict stresses values for a 2.5 mm diameter tungsten carbide spherical tip.

Ref. Value [MPa]	Relative to Yield Point	Predict Values		Difference Error	
σ_{ref} [MPa]	σ_{ref} / σ_y	σ_1 [MPa]	σ_2 [MPa]	$\sigma_{ref} - \sigma_1$ [MPa]	$(\sigma_{ref} - \sigma_1) / \sigma_{ref}$
0.0	0.0%	4.1	-5.2	-4.1	--
29.8	10.1%	23.2	-0.2	6.6	22.2%
58.1	19.7%	57.2	11.5	0.9	1.6%
88.7	30.1%	88.6	-3.5	0.0	0.0%
116.9	39.6%	125.9	2.1	-9.0	-7.7%
145.8	49.4%	147.7	-2.6	-1.9	-1.3%
177.1	60.0%	170.7	-1.4	6.4	3.6%
204.8	69.4%	200.9	0.0	4.0	1.9%
228.7	77.5%	230.8	0.2	-2.1	-0.9%

CONCLUSIONS

This paper investigates the possibility to quantify residual stresses combining the indentation method with a radial in-plane ESPI interferometer. The classical blind hole drilling mathematical model was modified by introducing three unknown parameters: ψ_1, ψ_2 and ψ_3. A set of well controlled experiments was designed to experimentally evaluate this measurement principle in only one material. Experimental data were fitted to this model and the resulting parameters were analyzed. A quadratic relationship was found between the residual stresses levels and the parameters ψ_1 and ψ_2. This relationship was used to predict residual stresses from the measured radial displacement field.

As a preliminary evaluation the results were considered very encouraging. It is clear that ψ_1 and ψ_2 in equations (9) and (10) are very good choices to be correlated with the residual stresses sum and differences respectively. The term ψ_3 seams to be more correlated to the indentation energy, and perhaps with material hardness, what can be very useful to verify the repeatability of the indentation device or the material's hardness homogeneity.

Both conic and spherical indentation tips shows about the same behavior. The values for ψ_1 and ψ_2 are obviously different for each tip geometry. Different conical angles or sphere radius must produce different values for ψ_1 and ψ_2. For the two tips investigated in this paper it was noted that the sensitivity for the spherical tip is higher than for the conical tip. The experimental data dispersion was smaller for the spherical tip. In addition, the amount of damage in the measured material's surface is smaller if a spherical tip is used.

The numerical results obtained in this investigation are very encouraging. It seams that is possible to quantify the residual stresses level without subtracting the radial displacement field of an indented stress-free material. Best results were found for stresses levels higher than 20% of the material's yield stress. In this work only stresses levels below 80% of the yield stress were investigated.

The maximum deviation between the predicted and reference stresses values are of about 8% for the spherical tip in the range of 20% to 80% of the yielding stresses. For the conical tip the difference was about the same, except for an outlier point the reached a difference of 17%.

Since only a one-axis stresses state was applied to the specimen, it was not possible to individually verify the dependence of ψ_1 and ψ_2 with the sum and difference between the principal stresses respectively. Although, since the absence of principal stresses difference produces only an axis-symmetrical phase difference pattern, it is clear that the principal stresses difference is responsible for introducing a dependence in terms of *cos(2θ)*, what is only related to ψ_2. So, ψ_1 is not affected by the principal stresses differences.

It has to be clear that these results are not definitive. Only one material was involved, only one-axis residual stresses induced was analyzed, only one energy level was used for the indentation. Further work will be focused on extending those conditions. Different materials and different residual stresses states are currently been investigated.

The final goal of this research work is to develop a portable residual stresses measurement unit. The authors believe that the combination of indentation and this radial in-plane ESPI interferometer can be the basis for a very practical device.

ACKNOWLEDGMENTS

The authors would like to thank the institutions that have been support this work: ANP-PRH34, CTPETRO, PADCT, CNPq/RHAE and CAPES.

REFERENCES

[1] ALBERTAZZI JR, A.; KANDA, C; BORGES, M. R.; HREBABETZKY, F. - ***"Portable Residual Stresses Measurement Device Using ESPI and a Radial In-Plane Interferometer"*** - Laser Metrology for Precision Measurement and Inspection in Industry; Albertazzi Jr., A.; Eds., Proc. SPIE, v. 4420, p. 112-122, Sep. 2001.

[2] GIANNAKOPOULOS, A. E.; SURESH, S. - ***"Indentation of Solids with Gradients in Elastic Properties. Part I: Point Force"*** - Journal of Solids and Structures, v.34, n.19, p.2357-2392, 1997.

[3] GIANNAKOPOULOS, A. E.; SURESH, A. - ***"Theory of Indentation of Piezoelectric Materials"*** - Elsevier Science Ltd., Acta Materialia, v.47 n.7 p.2153-2164, 1997.

[4] LU, JIAN - ***"Handbook on Measurement of Residual Stresses"*** - The Fairmont Press, SEM - Society for Experimental Mechanics, GA, USA, 1996.

[5] MAKINO, A.; NELSON D. - ***"Residual-Stress Determination by Single-Axis Holographic Interferometry and Hole Drilling. Part I: theory"*** - Exp. Mech. 34, 66-78 (1994).

[6] SUTERIO, R; ALBERTAZZI JR., A. G.; AMARAL, F. K.; - ***"Residual Stress Measurement using Indentation and a Radial ESPI Interferometer – Recent Progress"*** - ICEM12- 12th International Conference on Experimental Mechanics, Politecnico di Bari, Italy, 29 August - 2 September, 2004

[7] SUTERIO, R.; ALBERTAZZI JR., A. G.; PACHECO, A.; FERREIRA, R. P. - ***"Metrology Analysis of a Simulation Device for Residual Stress"*** (in Portuguese) - METROLOGIA 2003 – Brazilian Congress of Metrology, SBM –Brazilian Society of Metrology, Recife, PB, Brazil, sep. 1-5 , 2003.

[8] SUTERIO, R; ALBERTAZZI JR., A. G.; CAVACO, M. A. M. - ***"Preliminary Evaluation: The Indentation Method Combined with a Radial Interferometer for Residual Stress Measurement"*** - SEM Annual Conference and Exposition on Experimental and Applied Mechanics, SEM - Society for Experimental Mechanics, Charlotte, North Carolina, USA, June 2-4, 2003.

[9] UNDERWOOD, J. H. - ***"Residual Stress Measurement using Surface Displacements around an Indentation"*** - Experimental Mechanics, p. 373-380, Sep., 1973.